UNIVERSITY OF BIRMINGHAM
University of Birmingham Research at Birmingham

CC chemokine receptor 2 promotes recruitment of myeloid cells associated with insulin resistance in non-alcoholic fatty liver disease

Parker, Richard; Weston, Christopher J; Miao, Zhenhua; Corbett, Christopher; Armstrong, Matthew; Ertl, Linda; Ebsworth, Karen; Walters, Matthew; Baumart, Trageen; Newland, Dale; McMahon, Jeff; Zhang, Penglie; Singh, Rajinder; Campbell, James; Newsome, Philip N; Charo, Israel; Schall, Thomas; Adams, David H

DOI:
10.1152/ajpgi.00213.2017

License:
None: All rights reserved

Document Version
Peer reviewed version

Citation for published version (Harvard):
Parker, R, Weston, CJ, Miao, Z, Corbett, C, Armstrong, M, Ertl, L, Ebsworth, K, Walters, M, Baumart, T, Newland, D, McMahon, J, Zhang, P, Singh, R, Campbell, J, Newsome, PN, Charo, I, Schall, T & Adams, DH 2018, 'CC chemokine receptor 2 promotes recruitment of myeloid cells associated with insulin resistance in non-alcoholic fatty liver disease', *American journal of physiology. Gastrointestinal and liver physiology*, vol. 314, no. 4, pp. G483-G493. https://doi.org/10.1152/ajpgi.00213.2017

Link to publication on Research at Birmingham portal

Publisher Rights Statement:
Checked for eligibility: 15/03/2018
https://doi.org/10.1152/ajpgi.00213.2017

General rights
Unless a licence is specified above, all rights (including copyright and moral rights) in this document are retained by the authors and/or the copyright holders. The express permission of the copyright holder must be obtained for any use of this material other than for purposes permitted by law.

•Users may freely distribute the URL that is used to identify this publication.
•Users may download and/or print one copy of the publication from the University of Birmingham research portal for the purpose of private study or non-commercial research.
•User may use extracts from the document in line with the concept of 'fair dealing' under the Copyright, Designs and Patents Act 1988 (?)
•Users may not further distribute the material nor use it for the purposes of commercial gain.

Where a licence is displayed above, please note the terms and conditions of the licence govern your use of this document.

When citing, please reference the published version.

Take down policy
While the University of Birmingham exercises care and attention in making items available there are rare occasions when an item has been uploaded in error or has been deemed to be commercially or otherwise sensitive.

If you believe that this is the case for this document, please contact UBIRA@lists.bham.ac.uk providing details and we will remove access to the work immediately and investigate.

Download date: 27. Apr. 2024

CC Chemokine Receptor 2 Promotes Recruitment of Myeloid Cells Associated with Insulin Resistance in Non-Alcoholic Fatty Liver Disease

Richard Parker[1], Christopher Weston[1], Zhenhua Miao[2], Christopher Corbett[3], Matthew Armstrong[1], Linda Ertl[2], Karen Ebsworth[2], Matthew Walters[2], Trageen Baumart[2], Dale Newland[2], Jeff McMahon[2], Penglie Zhang[2], Rajinder Singh[2], James Campbell[2], Philip Newsome[1], Israel Charo[2], Thomas Schall[2], David H Adams[1]

1. NIHR Biomedical Research Unit and Centre for Liver Research, University of Birmingham, Birmingham, United Kingdom
2. ChemoCentryx Inc, Mountain View, California USA
3. Royal Wolverhampton Hospitals NHS Foundation Trust, Wolverhampton UK

Running head: CCR2 in NAFLD

Corresponding author:
Dr Richard Parker
richardparker@nhs.net
NIHR Centre for Liver Research
5th Floor IBR
University of Birmingham
Birmingham
B15 2TT
United Kingdom
Telephone (44) (0) 7971118036
Fax (44) (0) 121 415 8701

List of abbreviations

ALT	Alanine aminotransferase
ANOVA	Analysis of variance
AST	Aspartate aminotransferase
CCL2	CC chemokine ligand 2
CCR2	CC chemokine receptor 2
ELISA	Enzyme linked immunosorbent assay
FACS	Flow assisted cytometry
HFD	High fat diet
NAFLD	Non-alcoholic Fatty Liver Disease
NAS	NAFLD activity score
NASH	Non-alcoholic steatohepatitis
PBS	Phophate buffered saline
RNA	Ribonucleic acid
rt-PCR	Real time polymerase chain reaction
SEM	Standard error of mean

Financial Support: RP received support from a Clinical Research Training Fellowship from the Medical Research Council grant number G1100448, and a Sheila Sherlock Travelling Fellowship in Hepatology awarded by the Royal College of Physicians, London. ChemoCentryx Inc designed and developed the small molecule inhibitor of chemokine-C-receptor 2, CCX872, which is a proprietary compound.

Author contributions:

RP designed and performed experiments and analysis, wrote the draft manuscript
CW designed experiments, analysed data and reviewed the draft manuscript
CC collected human samples, performed experiments and reviewed the draft manuscript
MA collected samples and reviewed the draft manuscript
LE, KE, TB assisted with animal experiments
ZM, DN, JM, PZ, RS medicinal chemistry
MW, JC, PN, IC, TS and DA designed experiments, analysed data and reviewed the draft manuscript.
All authors reviewed the final manuscript and approved its submission

Conflicts of interest

RP: no conflict of interest
CW: no conflict of interest
CC: no conflict of interest
MA: no conflict of interest
LE: employee of ChemoCentryx Inc.
KE: employee of ChemoCentryx Inc.
TB: employee of ChemoCentryx Inc.
ZM: employee of ChemoCentryx Inc.
DN: employee of ChemoCentryx Inc.
JM: employee of ChemoCentryx Inc.
PZ: employee of ChemoCentryx Inc.
RS: employee of ChemoCentryx Inc.
MW: no conflicts of interest
JC: employee of ChemoCentryx Inc.
PN: no conflicts of interest
IC: employee of ChemoCentryx Inc.
TS: employee of ChemoCentryx Inc.
DA: no conflicts of interest

Abstract

Non-alcoholic fatty liver disease (NAFLD) is a common disease, closely associated with obesity and insulin resistance. We investigated the presence of a subset of myeloid cells associated with metabolic disturbance in the liver of patients with NAFLD and a murine model of obesity-induced liver disease. Gene and protein expression in liver and serum was investigated with rt-PCR or ELISA and correlated to clinical disease. Liver-infiltrating immune cells were isolated from normal or diseased human liver for flow cytometric analysis. In animal experiments, mice were fed a high-fat diet (60% of calories from fat) for 16 weeks, or high-fat diet with 30% fructose for 32 weeks to induce steatohepatitis and fibrosis. A small molecule inhibitor of CCR2, CCX872, was administered to some mice. A subset of $CD11c^+CD206^+$ immune cells were enriched in human liver tissue, and greater infiltration was observed in NAFLD. The presence of $CD11c^+CD206^+$ myeloid cells correlated with systemic insulin resistance. $CD11c^+CD206^+$ cells expressed high levels of CCR2, and liver CCL2 expression was increased in NASH and correlated with disease activity. In mice, CCR2 inhibition reduced infiltration of liver $CD11b^+CD11c^+F4/80^+$ monocytes, which are functional homologs of human $CD11c^+CD206^+$ cells, and improved liver injury and glycaemic control. A role for CCR2/CCL2 in human NAFLD has long been postulated. These data confirm a role for this chemokine/receptor axis, through mediating adipose and hepatic infiltration of myeloid cells. Inhibition of CCR2 improved hepatic inflammation and fibrosis in murine models of NAFLD. These data confirm the rationale for targeting CCR2 to treat NAFLD.

New and noteworthy

These data show for the first time that $CD11c^{+}CD206^{+}$ myeloid cells, previously associated with human adipose tissue inflammation, infiltrate into liver tissue in non-alcoholic fatty liver disease. These cells express CCR2. Inhibition of CCR2 in mice inhibits hepatic inflammation caused by a murine homolog of these myeloid cells and improves experimental liver disease.

Keywords:

1. Non-alcoholic fatty liver disease
2. Immunology
3. Obesity
4. Insulin resistance
5. Immunology

CC Chemokine Receptor 2 Promotes Recruitment of Myeloid Cells Associated with Insulin Resistance in Non-Alcoholic Fatty Liver Disease

Non-alcoholic fatty liver disease (NAFLD) covers a spectrum of liver pathology from hepatic steatosis (non-alcoholic fatty liver, NAFL) through the more severe non-alcoholic steatohepatitis (NASH) to cirrhosis (31). NAFLD is present in up to one-third of individuals (6) and is associated with the metabolic syndrome, particularly obesity (31) and insulin resistance (3). NAFLD is becoming the commonest indication for liver transplantation in the USA (32) reflecting both the prevalence of the disease and the present lack of effective therapies for advanced disease (25).

There is increasing interest in the role of the innate immune system in obesity and the metabolic syndrome. Myeloid cells infiltrate adipose and liver tissue in patients with NAFLD and secrete cytokines and adipokines that contribute to insulin resistance and inflammation. In particular, $CD11c^+CD206^+$ monocytes in human adipose tissue are associated with adipocyte necrosis, inflammation and insulin resistance (30). In mice, a functionally similar subset defined by $CD11b^+CD11c^+F4/80^+$ contribute to adipose inflammation and systemic insulin resistance in mice (22, 26). CCR2 mediates obesity-associated macrophage infiltration of adipose and hepatic tissue (19, 29). Mouse experiments have demonstrated that obesity increases hepatic expression of CCL2 (13, 14, 23, 29) and $CD11b^+CD11c^+F4/80^+$ express CCR2 (26). Inhibition of the CCR2/CCL2 axis reduces disease activity in mice (21, 27, 33)(4, 8). The CCR2/CCL2 axis in human NAFLD is less well defined, although increased circulating levels of CCL2 are observed (12, 14). We investigated the inflammatory infiltrate in human NAFLD and murine models of obesity-

induced liver disease to determine whether functionally important subsets of CCR2 inflammatory cells are involved in the metabolic dysfunction that characterises NAFLD.

Materials and methods

Human tissue

Human tissue and blood was collected from patients with liver disease or healthy controls at University Hospitals Birmingham NHS Foundation Trust with full informed consent and research ethics committee approval (REC reference 06/Q2708/11). Liver tissue was obtained from patients undergoing hepatic resection for benign or malignant disease, or liver transplantation for chronic liver disease. In the case of hepatic resection, liver tissue distal to resected lesions was used for analysis. No patient had undergone chemotherapy in the two weeks prior to surgery. Liver tissue was placed in formalin or snap frozen prior to subsequent analysis. Characteristics of these groups and of patients undergoing resection or transplantation as a source of liver tissue are detailed in **table 1**. Serum from patients with NAFLD was obtained from 2 cohorts of patients taking part in the LEAN and NOBLES studies. LEAN is a randomised controlled trial of liraglutide in patients with NAFLD (2). The serum samples used were taken before randomisation. NOBLES is an observational study of biomarkers in patients with liver disease. Finally, a group of healthy volunteers without liver disease donated blood for analysis and served as a control group in ELISA experiments. This group were drawn from laboratory colleagues and gave consent for their samples to be used for research.

Enzyme Linked Immunosorbent Assays (ELISA)

Analysis of human serum was performed using commercially available ELISA kits. Serum CCL2 concentration was measured using R&D Systems Quantikine kits (Minneapolis, Minnesota USA, catalogue number PDCP00), performed according to the manufacturer's instructions. Recombinant human chemokines were used as a positive control (Peprotech,

New Jersey USA). Samples were diluted in sample buffer 1:4 and run in duplicate. A standard curve was generated from known concentrations of recombinant chemokine and experimental values interpolated from this curve.

Polymerase Chain Reaction

RNA was isolated by homogenizing liver tissue in Trizol (Life Technologies, California, USA). Chloroform was added and samples centrifuged at top speed in a microfuge for 15 minutes. The upper aqueous layer was removed, isopropanol was added and samples centrifuged at 12,000rpm for 15 minutes. The resulting RNA pellet was washed in 70% ethanol and re-suspended in nuclease free water. Purity and concentration of total RNA was determined spectrophotometrically. cDNA was prepared from RNA using Taqman reagents (Life Technologies, California, USA) according to the manufacturer's instructions. Briefly, 2 μL of RNA was combined with random hexamers, reverse transcriptase, RNase inhibitor, magnesium chloride and a buffer solution. This mixture was heated to 25°C for 10 minutes, 37°C for 30 minutes, 95°C for 5 minutes and then cooled to 4°C. Probe/primer mixes for genes of interest and appropriate controls were obtained from Taqman (Life Technologies, California, USA) and made up with Taqman reagents. A 96 well plate was used for reactions, with wells containing cDNA, primer/probe mix (*CCL2* primer/probe mix catalogue number Hs00234140_m1, *18S* mix catalogue number Hs03003631_g1) and Taqman mastermix. Three replicates were used for both the gene of interest and housekeeping gene. *18S* has been shown to have lowest level of variability across stages of alcoholic liver disease (ALD) suggesting it is reliable as a housekeeping gene in steatohepatitis (5). PCR experiments were performed using a Roche Lightcycler 480 machine. A single quantification measurement was taken during each cycle.

Isolation of leukocytes

Isolation of leukocytes from human liver or blood

Mononuclear cells were isolated from blood or liver. Liver was washed with phosphate buffered saline (PBS) to remove blood and digested non-enzymatically using GentleMACS (Miltenyi). The resulting homogenate was passed through a sterile 70 micron mesh . The homogenate was then washed in PBS until a clear supernatant was achieved. Liver homogenate or whole blood was layered over a density gradient (Lypmhoprep, CedarLane Labs, Canada) to isolate mononuclear cells, which were aspirated from the interface and washed in PBS three times before further analysis.

Isolation of leukocytes from murine liver tissue

Mice were sacrificed by CO_2 inhalation and cervical dislocation. Blood samples were taken by left ventricular puncture. PBS was gently infused into the left ventricle to flush end organs of blood before harvesting. The liver were removed, immediately divided and placed into RPMI, formalin or snap frozen in liquid nitrogen. To isolate leukocytes, a segment of liver was coarsely chopped with scissors before mechanical dissociated by gently passing homogenate through a 75-micron sieve. The resulting homogenate was washed in PBS until a clear supernatant was achieved. For analysis of mouse liver, whole homogenate was incubated with fluorescently-tagged antibodies as described below, and CD45 used to identify leukocytes.

Flow Cytometry analysis of leukocytes

Isolated cells were suspended in 100μL at $1x10^6$ cells/ml in MACS buffer (PBS containing 2% FCS and 1mM EDTA) and incubated with antibodies. After incubation for 20 minutes at room temperature, cells were washed and re-suspended in PBS and analysed by flow cytometry using a Beckman Coulter Cyan. Cells stained with single colours were analysed for compensation and appropriate isotype controls were used to define the negative populations.

Animal experiments

Mouse experiments were performed at ChemoCentryx Inc, California, USA. C57/Bl6 mice were purchased from Charles River, USA, and were housed in the research locations for at least three days before investigations were started. Animals were housed according to local and national standards. Animal housing was maintained at 23°c with twelve hour light/dark cycles. Male C57/Black 6 (C57/Bl6) mice bred in controlled clean conditions were used for all experiments, aged 6-8 week at the start of experiments.

Two animal models were used: high fat diet (HFD) to induce steatohepatitis, or HFD in combination with 30% fructose in drinking water to induce steatohepatitis with fibrosis. The HFD provided 60% of calories from fat (by overall weight, this is provided 31% by lard and 3% by soybean oil). HFD and control diet were obtained from Teklad, USA. HFD was administered for 16 weeks; HFD+fructose was administered for 32 weeks. In each case, a control group of littermates were fed control diet (10% of calories from fat) with normal drinking water for the duration of the experiment. At the end of experiments mice were sacrificed by CO_2 inhalation.

Chemokine receptor antagonism

A small molecule inhibitor of CCR2 (CCX872) manufactured by ChemoCentryx Inc, Mountain View, USA. CCX872 was dissolved in 1% hydroxypropyl methylcellulose (HPMC) and administered to mice by subcutaneous injection at a dose of 30mg/kg daily. An equivalent volume of 1% HPMC was given in control experiments. A maximum volume of 350μL was used.

Triglyceride content of murine liver tissue

Triglyceride content of murine liver tissue was assessed using a commercially available colorimetric assay kit (Cayman Chemical Company, Ann Arbor MI USA) according to the manufacturer's instructions. In short, 400mg of liver tissue was suspended in 2ml of assay diluent and homogenised. 10μl of homogenate was added to wells of a 96 well plate, each sample was assayed in triplicate. Triglycerides were enzymatically hydrolysed to free fatty

acids and glycerol using the supplied enzyme mixture. After 15 minutes incubation colour change was measured with a plate reader (Synergy HT, BioTek, Vermont, USA) by measuring absorbance at 540nm. A standard curve was generated by assaying known concentrations of triglyceride and the triglyceride concentration of samples interpolated from this curve and expressed as milligram per gram of liver tissue.

Fibrosis content of liver tissue

Entire lobes of mouse livers were immersed in formalin immediately after harvesting and subsequently embedded in paraffin. Sections of10 μm thickness were stained with Sirius red (Sigma Aldrich, Missouri, USA) to detect collagen deposition. Briefly, sections were dewaxed and stained with haematoxylin before being stained with Sirius red for 1 hour. Sections were then dehydrated and mounted. Fibrosis was quantified by calculating percentage area of collagen deposition using Image-J software (National Institutes of Health, USA; version 1.48). Two Sirius red-stained slides per animal were taken at different depth, with 18 images taken randomly per slide for a total of 36 images per animal for collagen quantification. All pathologic evaluations were made by a pathologist on a random and blinded basis.

Glycaemic control

Glucose metabolism in mice was assessed with insulin and glucose challenge experiments. Insulin challenge was performed by administering 0.75U/kg of insulin (Sigma Aldrich, USA) to non-fasted mice via intra-peritoneal injection. Plasma glucose was measured with an AccuCheck glucometer (Roche, Basel, Switzerland) using a drop of blood from a tail vein. Plasma glucose was measured at baseline and 15, 30, 60, 90 and 120 minutes following administration of insulin. Mice were fasted overnight before glucose tolerance tests. Glucose (Sigma Aldrich, USA) was administered at 2g/kg of glucose (as 45% glucose solution), given by gastric lavage. Plasma glucose was measured at baseline and 15, 30, 60, 90 and 120 minutes after administration of glucose using an AccuCheck glucometer and drops of blood from tail vein.

Statistical Analysis

Data are expressed as mean and SEM for normally expressed data, and median and interquartile range (IQR) for skewed data. Normality was assessed with the Kolmogorov-Smirnov test. Normally distributed data were compared between groups with student's t-test, and the Mann-Whitney test used for skewed data. Variance across multiple groups, for example over a range of concentrations was analysed with one-way analysis of variance (ANOVA). Survival analysis was analysed by Kaplan-Meier curves with p values assessed with log-rank test. Median time to death in animals that died was also calculated. All authors had access to the study data and reviewed and approved the final manuscript. Data were analysed using Prism version 5 (California, USA).

Results

$CD14^+CD11c^+CD206^+$ monocytes are enriched in NAFLD liver tissue

Immune cells that express $CD14^+CD11c^+CD206^+$ have been detected in human adipose tissue and associated with insulin resistance (30). We examined the presence of these cells in human blood and liver. Liver tissue from patients with NAFLD (n=8), other liver disease (ALD n=4, PSC n=3, PBC n=2, cryptogenic cirrhosis n=1, haemochromatosis n=1) or without liver disease (n=5) was analysed. Very few $CD14^+CD11c^+CD206^+$ were observed in peripheral blood, whereas these cells were enriched in liver tissue (**figure 1**). The frequency of intrahepatic $CD11c^+CD206^+$ monocytes, as a percentage of $CD45^+CD14^+$ cells, differed significantly between types of liver disease (Kruskal-Wallis p=0.023) with highest frequency of cells seen in NAFLD (**figure 1E**). Mean fluorescence intensity (MFI) of CD11c and CD206 showed a tendency to be greater in NAFLD, although this did not reach statistical significant (Kruskal-Wallis p=0.056) (**figure 1F**). No differences in expression of CD11c and CD206 were seen between non-cirrhotic and cirrhotic liver tissue (data not shown).

279 CD14$^+$CD11c$^+$CD206$^+$ monocytes are associated with insulin resistance and express CCR2
280 in NAFLD
281 A correlation between the proportion of intrahepatic CD14$^+$CD11c$^+$CD206$^+$ monocytes
282 and glycosylated haemoglobin (HbA1c) was observed in liver infiltrating monocytes isolated
283 from patients with chronic liver disease (r^2 0.499 p=0.0005) (**figure 2A**). No significant
284 correlation was observed with age, BMI or ALT (**table 2**). In both blood and liver, CCR2
285 expression was largely restricted to CD14$^+$ monocytes particularly the classical
286 CD14^{++}CD16$^-$ subset (**figure 2B**). The overall frequency of CCR2$^+$ cells in blood or liver
287 tissue did not vary significantly by aetiology of liver disease (one-way ANOVA p=0.236).
288 However, CCR2$^+$ expression on CD14$^+$CD11c$^+$CD206$^+$ monocytes was higher in NAFLD
289 compared to normal liver tissue or non-NAFLD liver disease in terms of the percentage of
290 CD14$^+$CD11c$^+$CD206$^+$ cells that expressed CCR2 (**figure 3A)** and the MFI of CCR2
291 **(figure 3B).**

292 CCL2 is upregulated in NAFLD
293 *CCL2* gene expression in liver tissue was analysed by quantitative real-time PCR using *18S* as
294 a housekeeping gene. *CCL2* gene expression was significantly up regulated in liver tissue from
295 patients with NAFLD undergoing transplantation (Mann Whitney test p=0.009) (**figure 4A**).
296 The concentration of CCL2 was measured by ELISA in serum of individuals with biopsy-
297 proven NAFLD (n=20) or healthy volunteers (n=10). Serum CCL2 concentration was
298 significantly higher in patients with NAFLD compared to healthy volunteers (median
299 305.1pg/ml (IQR 211.8 – 385.7) vs. 224.7 (105.2 – 255.4), Mann-Whitney test p=0.021)
300 (**figure 4B**). NAFLD was assessed histologically by independent pathologists using the
301 NAFLD activity score (NAS) proposed by Kleiner and Brunt (15). Serum CCL2
302 concentration was higher in individuals with more severe histological inflammation (assessed
303 with the NAFLD activity score (NAS) (15))(one way ANOVA p=0.025) but levels did not
304 correlate with fibrosis stage (one way ANOVA p=0.347) (**figure 4C, D**). When
305 individual components of the NAS were considered, serum CCL2 concentration was

associated with higher lobular inflammation score (one-way ANOVA p=0.043) but not with steatosis or hepatocyte ballooning, consistent with the known role of CCL2 as a monocyte chemo-attractant.

Inhibition of CCR2 reduces accumulation of F4/80$^+$CD11c$^+$ monocytes in murine steatohepatitis

CD11b$^+$ CD11c$^+$F4/80$^+$ monocytes are found in adipose tissue in experimentally induced obesity in mice, and are functionally similar to CD11c$^+$CD206$^+$ monocytes in humans. To investigate the effect of CCR2 inhibition in obesity-induced steatohepatitis, twenty-six male C57/Bl6 mice were given HFD with 60% of calories from fat for 16 weeks. After eight weeks of HFD, the mice were divided into two groups: thirteen were treated daily with CCX872 (30mg/kg/day, administered by subcutaneous injection) and 13 received an equivalent volume of vehicle (1% HPMC). A further 8 littermates were given control diet for the duration of the experiment.

Steatosis, assessed by measuring triglyceride content of liver tissue, was markedly increased after 16 weeks of HFD. Mice treated with CCX872 had significantly less triglyceride accumulation in comparison with vehicle treated mice (169.6mg/g ±21.20 vs. 284.2 ±31.9, student's t-test p=0.007) with levels reduced to those seen in animals receiving a control diet (**figure 5A**). Serum ALT was significantly lower in CCX872-treated mice (mean ALT 252.5IU/ml ±56.02 vs. 532.8 ±98.07, student's t-test p=0.028) (**figure 5B**). The reduction in hepatic steatosis was confirmed histologically (**figure 5C**) but histological features of inflammation and fibrosis did not differ between groups (**figure 5D, E**).

Flow cytometric analysis of isolated liver-infiltrating immune cells revealed an increase in CD11b$^+$F4/80^{low} cells in all HFD fed mice. No differences were seen between groups with regard to intrahepatic frequencies of CD11b$^+$F4/80^{hi} Kupffer cells or overall CD11b$^+$F4/80^{low} infiltrating monocytes (**figure 6A, B**). However, fewer CCR2 expressing monocytes were seen in CCX872 treated mice (**figure 7A**) and CCR2 inhibition reduced liver infiltration with Ly6c^{hi} monocytes (**figure 7B**). HFD feeding resulted in higher intrahepatic and adipose

tissue frequencies of $CD11b^+$ $CD11c^+F4/80^+$ cells, an immune cell population functionally similar to $CD11c^+CD206^+$ cells in humans which are implicated in the development of obesity mediated insulin resistance (19). The frequency of $CD11b^+CD11c^+F4/80^+$ cells in both adipose and liver tissue was significantly reduced after treatment with CCX872 (**figure 6C, D**).

Inhibition of CCR2 reduces scarring in murine steatohepatitis and fibrosis

Only mild hepatic fibrosis was seen after 16 weeks of HFD (figure 7E). As fibrosis is an important prognostic marker in human NAFLD (1, 9) we sought to assess the effects of CCR2 antagonism on the development of fibrosis. Fructose intake is associated with more severe fibrosis in human NAFLD (24) and has been shown to cause fibrosis in animal models of NAFLD (7, 16). We used HFD and fructose to induce fibrosis and assess the effect of CCR2 antagonism. Twenty-two mice were given HFD and 30% fructose for 32 weeks. CCX872 or vehicle was administered daily for the final eight weeks of the experiment, each to 11 mice. A further four littermates were given control diet for the duration of the experiment.

Consistent with initial experiments, after 32 weeks lower ALT concentrations were observed in CCX872-treated animals (median 67.0 IU/L vs. 251.5IU/L, $p<0.006$ by Mann Whitney test) although interestingly, lower than seen after a shorter period of HFD diet alone. Hepatic fibrosis, assessed by area of scarring on histology, was significantly reduced in the livers of mice receiving CCX872 (mean area 0.83 % (SD 0.22) vs. 2.01 (1.5), $p=0.01$ by student's t-test) (**figure 8**).

CCR2 antagonism improves glucose metabolism in mice given HFD

At the start of the treatment period (after eight weeks of HFD), response to a glucose load was similar between CCX872 and vehicle treated mice (**figure 9A, C**). However, after 8 weeks of treatment there was a significant improvement in response of CCX872 mice compared to vehicle treated mice (AUC 48545 mg/dl/min vs. 31795 mg/dl/min, student's t-

359 test p<0.001) (**figure 9B, C**). Insulin challenge was performed by administering a standard
360 dose of 0.75units/g of insulin by intra-peritoneal injection to non-fasted mice. At the start of
361 the treatment period changes in plasma glucose concentration in response to insulin were
362 similar in both groups of mice fed HFD (**figure 9D, F**). After a further 8 weeks of HFD and
363 treatment with CCX872 or vehicle, there was a significant difference between groups (AUC
364 21719 mg/dl/min vs. 16553 mg/dl/min, student's t-test p<0.001) (**figure 9D,F**).

365 **Discussion**

366 Non-alcoholic fatty liver disease is a common condition closely related to obesity and the
367 metabolic syndrome. Progressive disease is typified by hepatic inflammation in the form of
368 steatohepatitis and fibrosis (11). We report here that a subset of monocytes that express
369 both CD11c and CD206 are enriched in the liver of patients with NAFLD and their
370 presence is associated with insulin resistance. A similar subset has been reported previously
371 in human adipose tissue but not in liver tissue (30). We show that intrahepatic
372 $CD11c^{+}CD206^{+}$ monocytes express CCR2, and it principal ligand, CCL2, is over-expressed
373 in NAFLD liver tissue suggesting that the CCR2/CCL2 axis may promote trafficking of
374 $CD11c^{+}CD206^{+}$ monocytes to the liver in NAFLD which would suggest targeting CCR2
375 therapeutically may be of benefit in NAFLD.
376
377 To test this hypothesis we investigated the role of CCR2 in trafficking of pro-inflammatory
378 myeloid cells in a mouse model of non-alcoholic fatty liver disease where high fat diet feeding
379 causes insulin resistance, steatohepatitis and hepatic fibrosis. When a small molecule
380 inhibitor of CCR2 was administered to mice the numbers of liver and adipose tissue
381 infiltrating $CD11b^{+}CD11c^{+}F4/80^{+}$ cells was reduced, accompanied by improvements in liver
382 histology and glycaemic control.
383

The transition from simple steatosis to NASH is associated with hepatic inflammation and the development of insulin resistance even in the absence of overt diabetes mellitus. The present study suggests that a specific subset of liver tissue infiltrating monocytes provide the link between hepatic inflammation and insulin resistance. Wentworth at el. reported that the presence of pro-inflammatory $CD11c^{+}CD206^{+}$ monocytes in subcutaneous and omental adipose tissue of obese individuals (30) was associated with insulin resistance. This was mediated in part through the inhibition of the action of insulin on adipocytes. We now report the same subset of monocytes in the livers of patients with NASH. In contrast to Wentworth we detected high levels of CCR2 on $CD11c^{+}CD206^{+}$ cells in the liver. A comparable subset of monocytes in mice is defined by F4/80 and CD11c expression. These cells express CCR2 and use it to infiltrate adipose tissue (19). Our data confirm and extend these observations by showing that pharmacological inhibition of CCR2 reduces not only adipose tissue infiltration but also hepatic infiltration by this subset. A crucial role for these cells in disease pathogenesis was suggested by our finding of a strong correlation between the frequency of $CD11c^{+}CD206^{+}$ cells in the liver and clinical measurement of insulin resistance. Thus local hepatic insulin resistance may be mediated in part through inflammation caused by this monocyte subset recruited to the liver in response to increased CCL2 expression. Thus, the improvement in glucose metabolism observed in mice is likely to be multi-factorial. Improved adipose tissue inflammation will improves insulin resistance at this site, while reduced hepatic inflammation is also likely to improve hepatic glucose metabolism.

There have been several studies that examine the CCR2/CCL2 axis in the murine models of liver disease Inhibition of CCR2/CCL2 either through genetic manipulation (23, 29) or pharmaceutical targeting (4, 17, 21, 27, 33) leads to improvements in steatosis, inflammation or fibrosis with variation dependent on the model employed. Many of these pre-clinical pharmaceutical studies have relied on transgenic mice (28, 33) used

410 non-physiological methods such as administration of carbon tetrachloride (4) or
411 streptozotocin (17), or deficient diets (4, 21) and as such are of limited translational value.
412 Our data presented here deliberately used diets that mimic high-fat and /or high-
413 carbohydrate diets which are a feature of human liver disease. This is a particular contrast to
414 the study by Lefebvre et al (17) who induced NASH in part by using streptotozin to kill
415 pancreatic islet cells.
416
417 Increased CCL2 expression in human NAFLD has been described previously by Haukeland
418 et al. (12) who reported higher levels of circulating CCL2 in NAFLD and in progressive
419 disease. Our data confirm this finding and by correlating CCL2 blood levels with histological
420 features seen on liver biopsies taken at the same time show that CCL2 expression
421 correlates with hepatic inflammation but not fibrosis. We also show increased liver-specific
422 expression of CCL2 in patients with NAFLD although this data has limitations through the
423 number of samples used for analysis of liver-specific CCL2 expression, and the necessary
424 reliance of samples from patients with advanced disease to analyse liver inflammation. CCL2
425 is the major chemokine ligand for the receptor CCR2 which mediates myeloid cell trafficking
426 into tissues. Intrahepatic monocytes as a group express low levels of CCR2 but this is not
427 the case for $CD11c^{+}CD206^{+}$ monocytes which maintain high levels of CCR2 suggesting that
428 CCL2/CCR2 interactions may be more important for the recruitment and positioning of
429 these cells in liver tissue. Based on these findings we hypothesised that inhibiting CCR2
430 would reduce transmigration of monocytes into adipose and liver tissue. This was confirmed
431 in mice where inhibition of CCR2 using a small molecule CCR2 inhibitor reduced
432 accumulation of the corresponding murine subset of monocytes associated with reduced
433 steatohepatitis and improved metabolic parameters. Several studies have reported on the
434 use of a variety of pharmaceutical inhibitors of CCR2 in murine fatty liver disease,
435 administered in a variety of routes and in a variety of disease models (21, 27, 33). The
436 human data presented here confirm that CCR2 antagonism may be of benefit in

NAFLD and indeed a phase II trial of a joint CCR2/CCR5 inhibitor, cencriviroc, reported in 2016 showing benefit on hepatic fibrosis (10). The recently published results of the dual CCR2/CCR5 inhibitor, cencriviroc, in clinical NAFLD show some changes in inflammatory activity and encouraging improvements in fibrosis compared to placebo treatment. The most obvious difference between CCX872 and cencriviroc is the additional effect on CCR5 which may bring additional benefits in the setting of liver disease. Interestingly when cenicriviroc was compared to CCX872 in the methinone-choline deficient diet model of steatohepatitis, greater improvement in ALT and fibrosis was observed with CCX872 (20), although the MCD is not noted for causing a great deal of fibrosis and also lacks relevance to human NAFLD. CCR2 antagonists have been used in clinical trials in a variety of diseases where their use seems safe. Treatment of NAFLD would likely require administration over at least months and possibly years, and as such long-term safety is important. One important aspect of long-term use is the impact of CCR2 inhibition on carcinogenesis. Any effects are difficult to predict at present as animal models yield conflicting data (18), and CCR2 inhibition is being trialled for use in for example pancreatic cancer.

In conclusion, we suggest that a particular subset of monocytes is associated with progressive disease non-alcoholic fatty liver disease and that infiltration of liver by this subset is driven at least in part by CCL2/CCR2 signalling. Inhibition of this axis in NAFLD may be a rational means of improving hepatic and adipose tissue inflammation to prevent progressive liver disease.

References

1. Angulo, P. et al. Liver Fibrosis, but no Other Histologic Features, Associates with Long-term Outcomes of Patients With Nonalcoholic Fatty Liver Disease. Gastroenterology 2015

2. Armstrong, M. J. et al. Liraglutide efficacy and action in non-alcoholic steatohepatitis (LEAN): study protocol for a phase II multicentre, double-blinded, randomised, controlled trial. BMJ open 2013;3(11):e003995.

3. Armstrong, M. J. et al. Abdominal subcutaneous adipose tissue insulin resistance and lipolysis in patients with non-alcoholic steatohepatitis. Diabetes Obes Metab 2014;16(7):651-660.
4. Baeck, C. et al. Pharmacological inhibition of the chemokine CCL2 (MCP-1) diminishes liver macrophage infiltration and steatohepatitis in chronic hepatic injury. Gut 2012;61(3):416-426.
5. Boujedidi, H. et al. Housekeeping gene variability in the liver of alcoholic patients. Alcoholism: Clinical and Experimental Research 2012;36(2):258-266.
6. Browning, J. D. et al. Prevalence of hepatic steatosis in an urban population in the United States: impact of ethnicity. Hepatology 2004;40(6):1387-1395.
7. Charlton, M. et al. Fast food diet mouse: novel small animal model of NASH with ballooning, progressive fibrosis, and high physiological fidelity to the human condition. American Journal of Physiology-Gastrointestinal and Liver Physiology 2011;301(5):G825-G834.
8. Cynis, H. et al. Inhibition of Glutaminyl Cyclases alleviates CCL2-mediated inflammation of non-alcoholic fatty liver disease in mice. Int J Exp Pathol 2013;94(3):217-225.
9. Ekstedt, M. et al. Fibrosis stage is the strongest predictor for disease-specific mortality in NAFLD after up to 33 years of follow-up. Hepatology 2014
10. Friedman, S. L. et al. Antifibrotic effects of the dual CCR2/CCR5 antagonist cenicriviroc in animal models of liver and kidney fibrosis. HEpatology 2017e0158156.
11. Gadd, V. L. et al. The portal inflammatory infiltrate and ductular reaction in human nonalcoholic fatty liver disease. Hepatology 2014;59(4):1393-1405.
12. Haukeland, J. W. et al. Systemic inflammation in nonalcoholic fatty liver disease is characterized by elevated levels of CCL2. Journal of hepatology 2006;44(6):1167-1174.
13. Kanda, H. et al. MCP-1 contributes to macrophage infiltration into adipose tissue, insulin resistance, and hepatic steatosis in obesity. Journal of Clinical Investigation 2006;116(6):1494-1505.
14. Kirovski, G. et al. Elevated systemic monocyte chemoattractrant protein-1 in hepatic steatosis without significant hepatic inflammation. Exp Mol Pathol 2011;91(3):780-783.
15. Kleiner, D. E. et al. Design and validation of a histological scoring system for nonalcoholic fatty liver disease. Hepatology 2005;41(6):1313-1321.
16. Kohli, R. et al. High-fructose, medium chain trans fat diet induces liver fibrosis and elevates plasma coenzyme Q9 in a novel murine model of obesity and nonalcoholic steatohepatitis. Hepatology 2010;52(3):934-944.
17. Lefebvre, E. et al. Antifibrotic Effects of the Dual CCR2/CCR5 Antagonist Cenicriviroc in Animal Models of Liver and Kidney Fibrosis. PLoS One 2016;27 (11)
18. Li, M. et al. A role for CCL2 in both tumor progression and immunosurveillance. Oncoimmunology 2013

19. Lumeng, C. N., Bodzin, J. L., and Saltiel, A. R. Obesity induces a phenotypic switch in adipose tissue macrophage polarization. Journal of Clinical Investigation 2007;117(1):175-184.
20. Miao, Z. et al. Reduction of Liver Fibrosis by CCR2 antagonist CCX872 in Murine Models of NASH. Hepatology 2016;S1
21. Miura, K. et al. Hepatic recruitment of macrophages promotes nonalcoholic steatohepatitis through CCR2. Am J Physiol Gastrointest Liver Physiol 2012;302(11):G1310-21.
22. Nguyen, M. T. A., Favelyukis, S., and Nguyen…, A. K. A subpopulation of macrophages infiltrates hypertrophic adipose tissue and is activated by free fatty acids via Toll-like receptors 2 and 4 and JNK-dependent …. Journal of Biological … 2007
23. Obstfeld, A. E. et al. CC chemokine receptor 2 (CCR2) regulates the hepatic recruitment of myeloid cells that promote obesity-induced hepatic steatosis. Diabetes 2010;59(4):916-925.
24. Ouyang, X. et al. Fructose consumption as a risk factor for non-alcoholic fatty liver disease. Journal of hepatology 2008;48(6):993-999.
25. Parker, R., Hodson, J., and Rowe, I. A. C. Systematic Review: Current Evidence in Non-Alcoholic Fatty Liver Disease Lacks Relevance to Patients with Advanced Fibrosis. Journal of Gastroenterology and hepatology 2016
26. Patsouris, D. et al. Ablation of CD11c-positive cells normalizes insulin sensitivity in obese insulin resistant animals. Cell metabolism 2008;8(4):301-309.
27. Tamura, Y. et al. CC chemokine receptor 2 inhibitor improves diet-induced development of insulin resistance and hepatic steatosis in mice. Journal of atherosclerosis and thrombosis 2010;17(3):219-228.
28. Tamura, Y. et al. Inhibition of CCR2 ameliorates insulin resistance and hepatic steatosis in db/db mice. Arteriosclerosis, thrombosis, and vascular biology 2008;28(12):2195-2201.
29. Weisberg, S. P. et al. CCR2 modulates inflammatory and metabolic effects of high-fat feeding. Journal of Clinical Investigation 2006;116(1):115-124.
30. Wentworth, J. M. et al. Pro-inflammatory CD11c+ CD206+ adipose tissue macrophages are associated with insulin resistance in human obesity. Diabetes 2010;59(7):1648-1656.
31. Williams, C. D. et al. Prevalence of nonalcoholic fatty liver disease and nonalcoholic steatohepatitis among a largely middle-aged population utilizing ultrasound and liver biopsy: a prospective study. Gastroenterology 2011;140(1):124-131.
32. Wong, R. J., Cheung, R., and Ahmed, A. Nonalcoholic steatohepatitis is the most rapidly growing indication for liver transplantation in patients with hepatocellular carcinoma in the US. Hepatology 2014;59(6):2188-2195.
33. Yang, S. J. et al. Inhibition of the chemokine (C–C motif) ligand 2/chemokine (C–C motif) receptor 2 pathway attenuates hyperglycaemia and inflammation in a mouse model of hepatic steatosis and lipoatrophy. Diabetologia 2009;52(5):972-981.

Table 1: characteristics of cohorts used for human studies

	Age Years	**BMI** Kg/m^2	**ALT** IU/L	**Diabetes** prevalence
Serum				
NOBLES	55.1	33.9	56.1	58%
LEAN	51.0	36.0	71.5	33%
Liver tissue				
NASH cirrhosis	56.9	32.7	37.5	88%
non-NASH cirrhosis	55.3	29.3	34.1	14%
Normal	57.5	27.3	20.0	0%

Table 2: correlation of frequency of intrahepatic $CD11c^+CD206^+$ monocytes with clinical parameters

	Correlation with intrahepatic $CD11c^+CD206^+$ monocytes (as % of $CD14^+$) (r^2)	p value
HbA1c	0.50	<0.001
ALT	0.02	0.551
BMI	0.04	0.388
Age	0.16	0.084

Figure legends

Figure 1: $CD11c^+CD206^+$ monocytes are enriched in liver tissue. **A**, **B** gating strategy to identify $CD45^+CD14^+$ monocytes. Representative samples of (**C**) peripheral blood and (**D**) liver infiltrating monocytes from the same individual (**E**). Liver tissue from patients with NAFLD (n=8) showed a greater proportion of $CD11c^+CD206^+$ monocytes as a proportion of $CD45^+CD14^+$ monocytes, compared to other chronic liver disease (ALD n=4, PSC =3, PBC n=2, haemochromotosis n=1, cryptogenic cirrhosis n=1) or normal liver (n=5) (*$p<0.05$ by Kruskal-Wallis). (**F**) Mean fluorescence intensity of $CD11c^+CD206^+$ cells by liver disease (Kruskal-Wallis $p=0.056$).

Figure 2: Monocytes were isolated from liver tissue from patients with or without NAFLD and analysed by flow cytometry. **A** The frequency of CD11c+CD206+ monocytes in liver tissue correlated with insulin resistance, measured by HbA1c. n=24, r2 = 0.499. **B** CCR2 percentage expression was greater on CD14++CD16- monocytes with a non-significant reduction of CCR2 expression on all intra-hepatic monocytes.

Figure 3: Monocytes were isolated from liver tissue and analysed by flow cytometry. CCR2 expression was higher on $CD11c^+CD206^+$ monocytes isolated from NAFLD liver tissue (n=8) compared to non-NAFLD cirrhosis (n=11) or normal liver tissue (n=5) with regard to **A** percentage of $CCR2^+$cells (normal, median 39.4% IQR 40.1, non-NAFLD cirrhosis 59.7% IQR 24.9, NAFLD 80.1% IQR 24.7) **and** mean fluorescent intensity (normal 171 IQR 163.7, non-NAFLD cirrhosis 200.6 IQR 80.1, NAFLD 3299 IQR 144.4). Data shown as median and IQR, n=23 in each case. *$p<0.05$ by Mann-Whitney test

582 **Figure 4**: **A** RNA was isolated from liver tissue and CCL2 gene expression analysed by
583 semi-quantitative PCR. CCL2 gene expression was significantly increased in liver tissue from
584 patients with NASH (n=6) compared to normal liver tissue (n=6) (Mann Whitney test
585 $p<0.01$). **B** Serum concentration of CCL2 measured by ELISA was higher in NAFLD (n=20)
586 compared to healthy volunteers (n=10) (Mann Whitney test $p<0.05$) **C** serum concentration
587 of CCL2 increased with increasing disease activity as measured by the NAS score (one way
588 ANOVA $p<0.05$) **D** no relation was seen with fibrosis stage (one way ANOVA $p>0.05$)
589
590 **Figure 5**: Improvements in steatohepatitis with inhibition of CCR2. Thirteen animals in each
591 group were given HFD with daily administration of vehicle or CCX872, and a further 8
592 animals were given a control diet for 16 weeks. Triglyceride content was measured with a
593 colorimetric assay. CCR2 inhibition reduced triglyceride accumulation (*$p<0.05$, **$p<0.01$ by
594 students t-test). B CCR2 inhibition reduced serum ALT (*$p<0.05$ by student's t-test).
595 Histological assessment of liver disease confirmed reduced steatosis, as assessed by area of
596 staining, panel C, but no differences in D histological inflammation or E histological fibrosis
597
598 **Figure 6**: Myeloid cells from liver and adipose tissue from mice given a high fat diet were
599 analysed by flow cytometry. Treatment with a small molecule inhibitor of CCR2 did not
600 affect proportions of **A** intrahepatic Cd11b+F4/80hi Kupffer cells or **B** overall infiltrating
601 CD11b+F4/80low monocytes (Mann-Whitney test to compare vehicle and CCX872 groups,
602 *$p>0.05$). CCR2 antagonism reduced infiltration of CD11c+F4/80+ cells into **C** liver tissue
603 (Mann-Whitney test to compare vehicle and CCX872 groups, * $p<0.05$) and **D** adipose
604 tissue (Mann-Whitney test to compare vehicle and CCX872 groups, t-test $p<0.05$). Data are
605 shown as boxes to denote IQR with line at median and whiskers showing maximum and
606 minimum values.
607

608 **Figure 7**: Myeloid cells from liver and adipose tissue from mice given a high fat diet
609 were analysed by flow cytometry. Treatment with a small molecule inhibitor of CCR2
610 reduced hepatic infiltration with $CCR2^{+}$ $CD11b^{+}F4/80^{lo}$ monocytes (student's t-test
611 $p<0.05$) and **B** infiltration of liver tissue by pro-inflammatory $Ly6c^{hi}$ cells (**$p<0.05$ by
612 student's t-test)
613
614 **Figure 8**: 22 C57/Bl6 mice were fed HFD with 30% fructose in drinking water, or control
615 diet without fructose, for 32 weeks. CCR2 antagonism with a small molecule inhibitor,
616 CCX872, reduced fibrosis compared to vehicle control. Representative pictures of liver
617 sections from **A** control and **B** CCX872-treated animals. **C** Fibrosis as assessed by
618 percentage collagen area by Sirius red staining of liver sections. Data are shown as mean and
619 SEM **$p<0.05$ by student's t-test
620
621 **Figure 9**: CCR2 antagonism improved glycaemic control in mice on a HFD with CCR2.
622 Glycaemic control was assessed at the beginning and end of the treatment period
623 with glucose tolerance tests and insulin challenges. Mice in each group were showed
624 similar responses at the start of the treatment period (A, D). At the time of sacrifice
625 mice treated with CCX872 showed significantly improved response to glucose and
626 insulin (B, E). When assessed by measuring area under the curve statistically
627 significant changes were seen (C, F). ***$p<0.001$ by student's t-test.
628
629
630
631
632

633

634

635

636

637

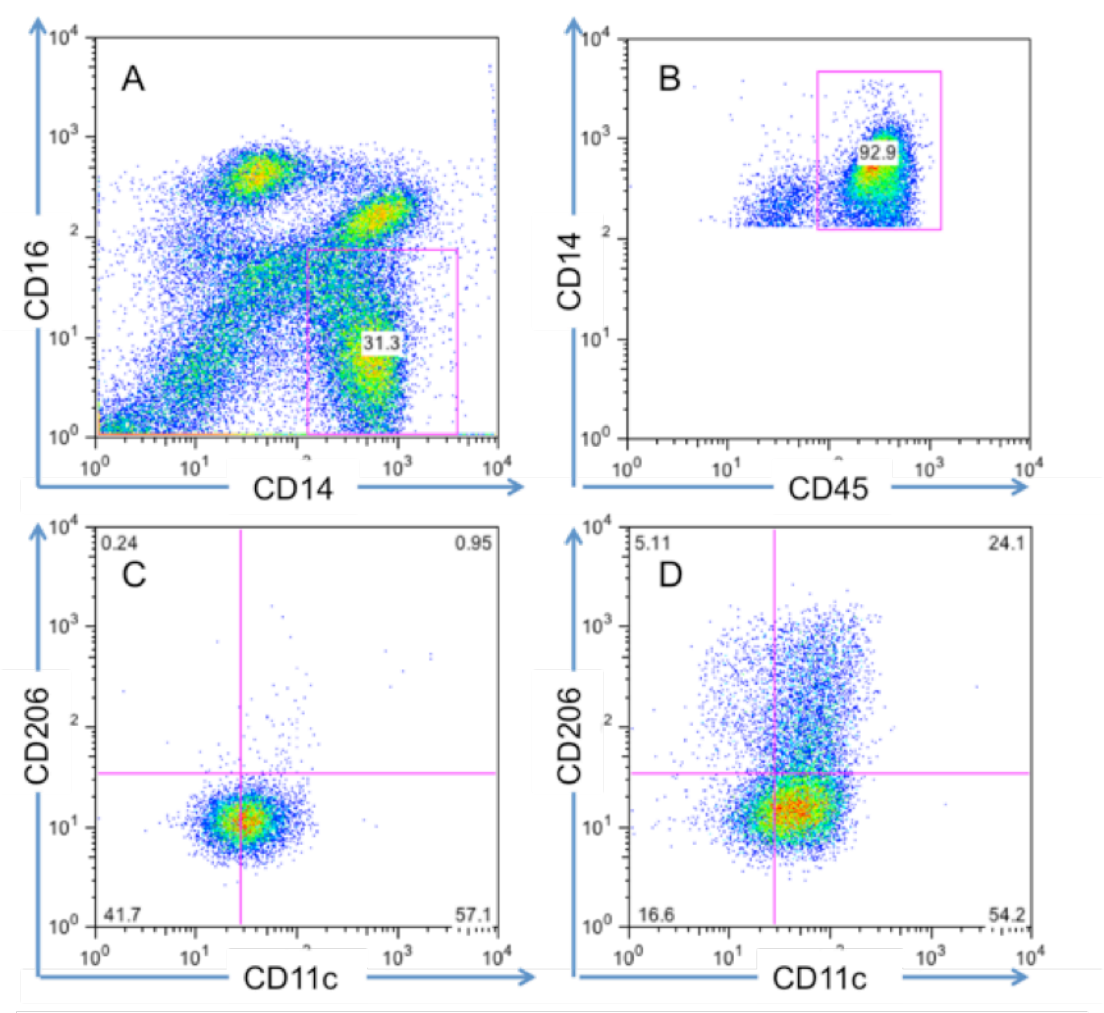

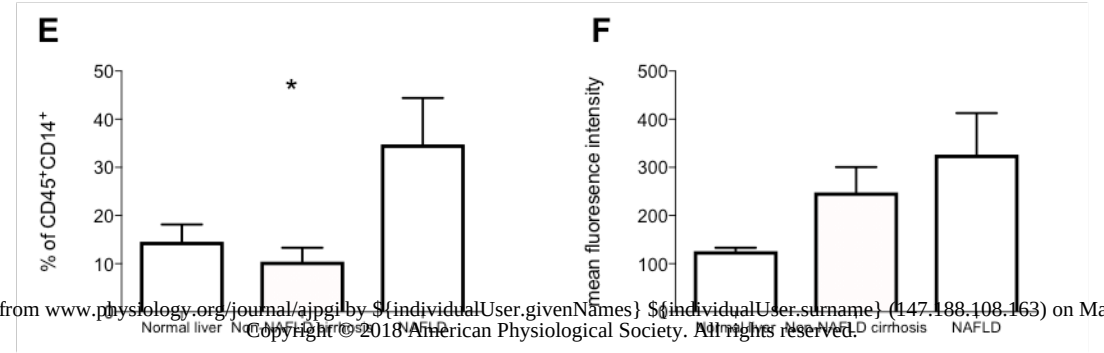

from www.physiology.org/journal/ajpgi by ${individualUser.givenNames} ${individualUser.surname} (147.188.108.163) on Ma
Copyright © 2018 American Physiological Society. All rights reserved.

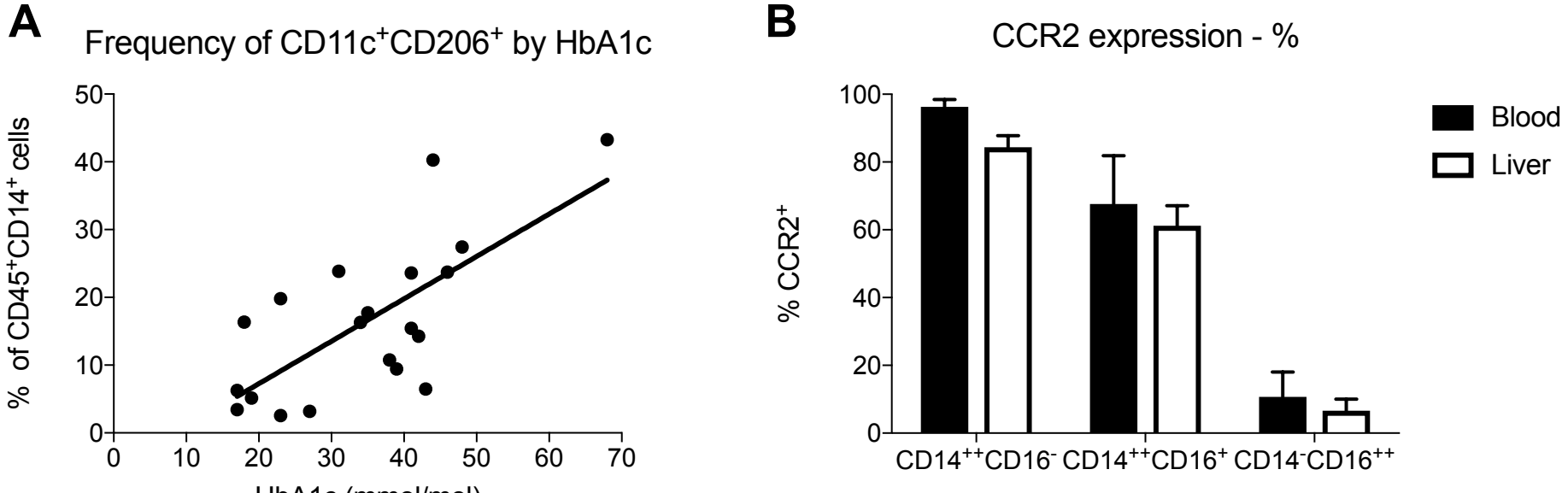

Downloaded from www.physiology.org/journal/ajpgi by ${individualUser.givenNames} ${individualUser.surname} (147.188.108.163) on March 15, 2018.
Copyright © 2018 American Physiological Society. All rights reserved.

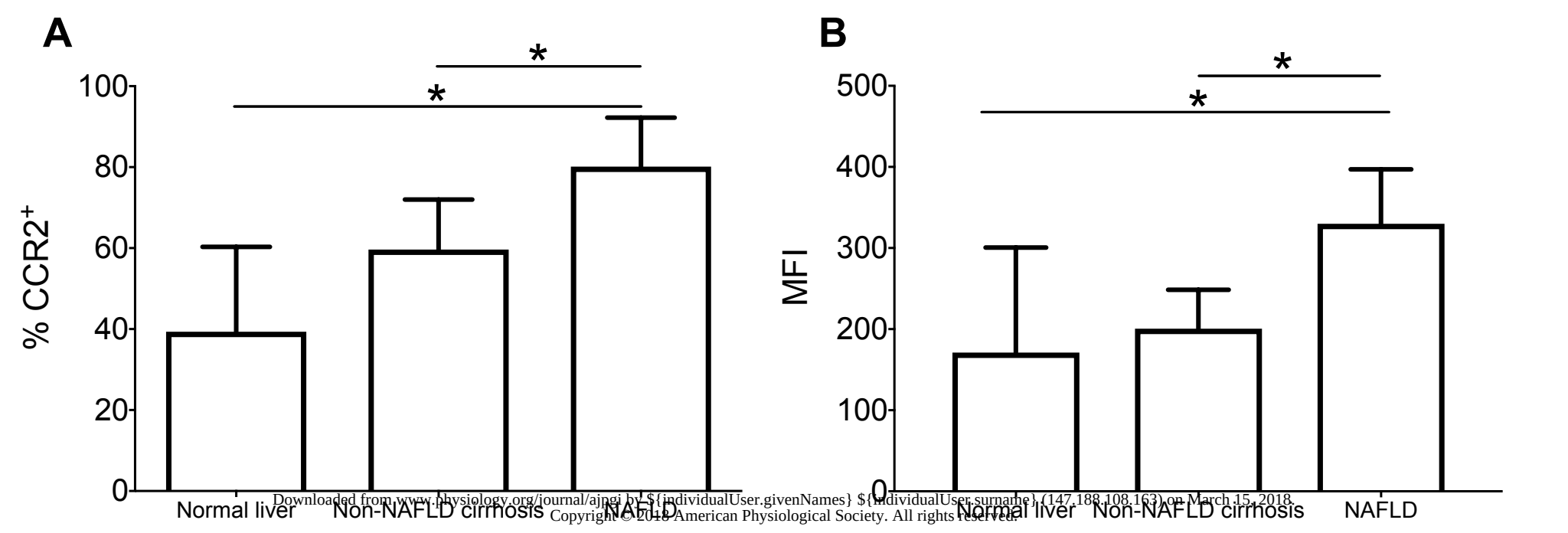

Downloaded from www.physiology.org/journal/ajpgi by ${individualUser.givenNames} ${individualUser.surname} (147.188.108.163) on March 15, 2018.
Copyright © 2018 American Physiological Society. All rights reserved.

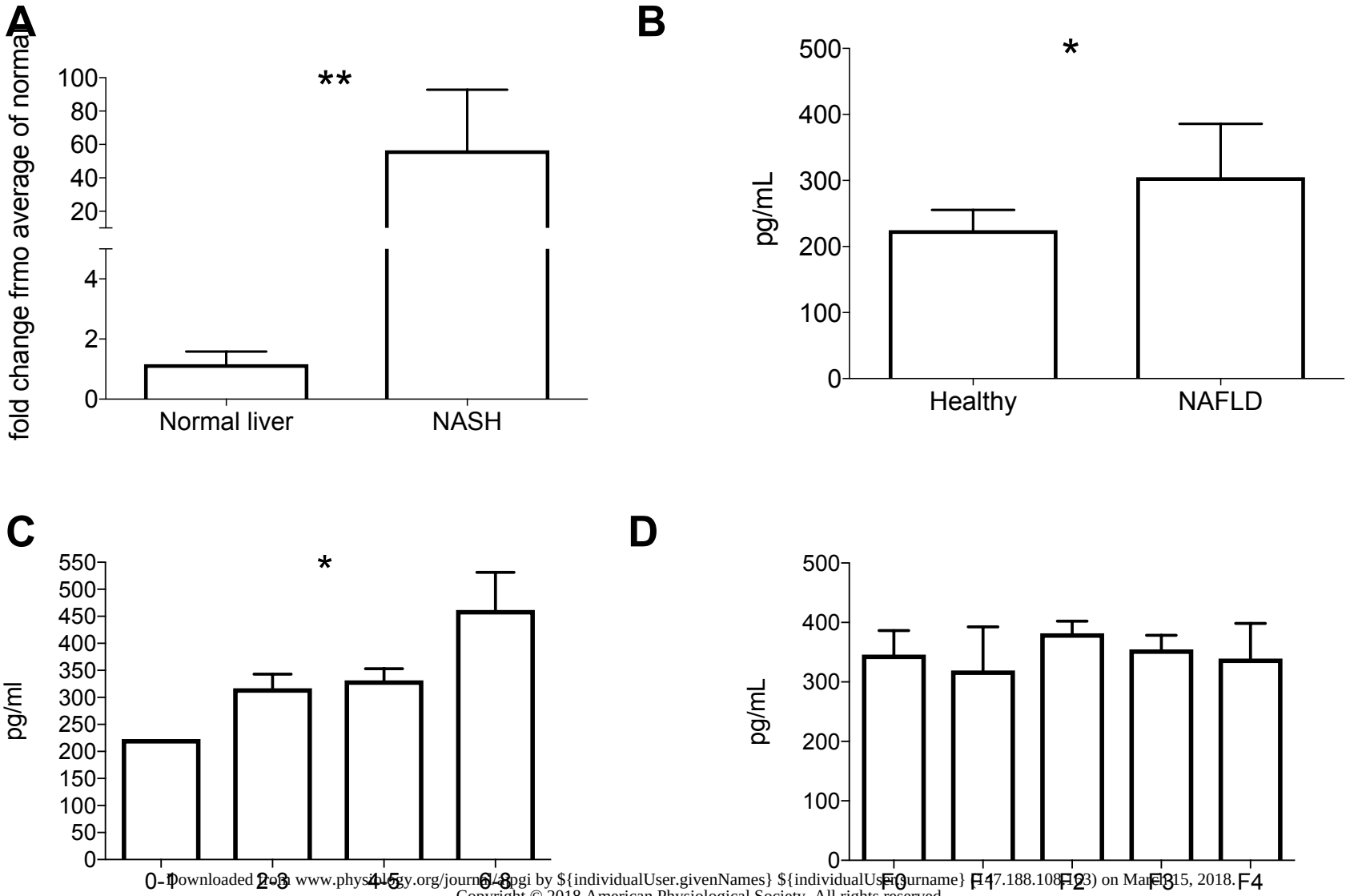

Downloaded from www.physiology.org/journal/ajpgi by ${individualUser.givenNames} ${individualUser.surname} (147.188.108.123) on March 15, 2018.
Copyright © 2018 American Physiological Society. All rights reserved.

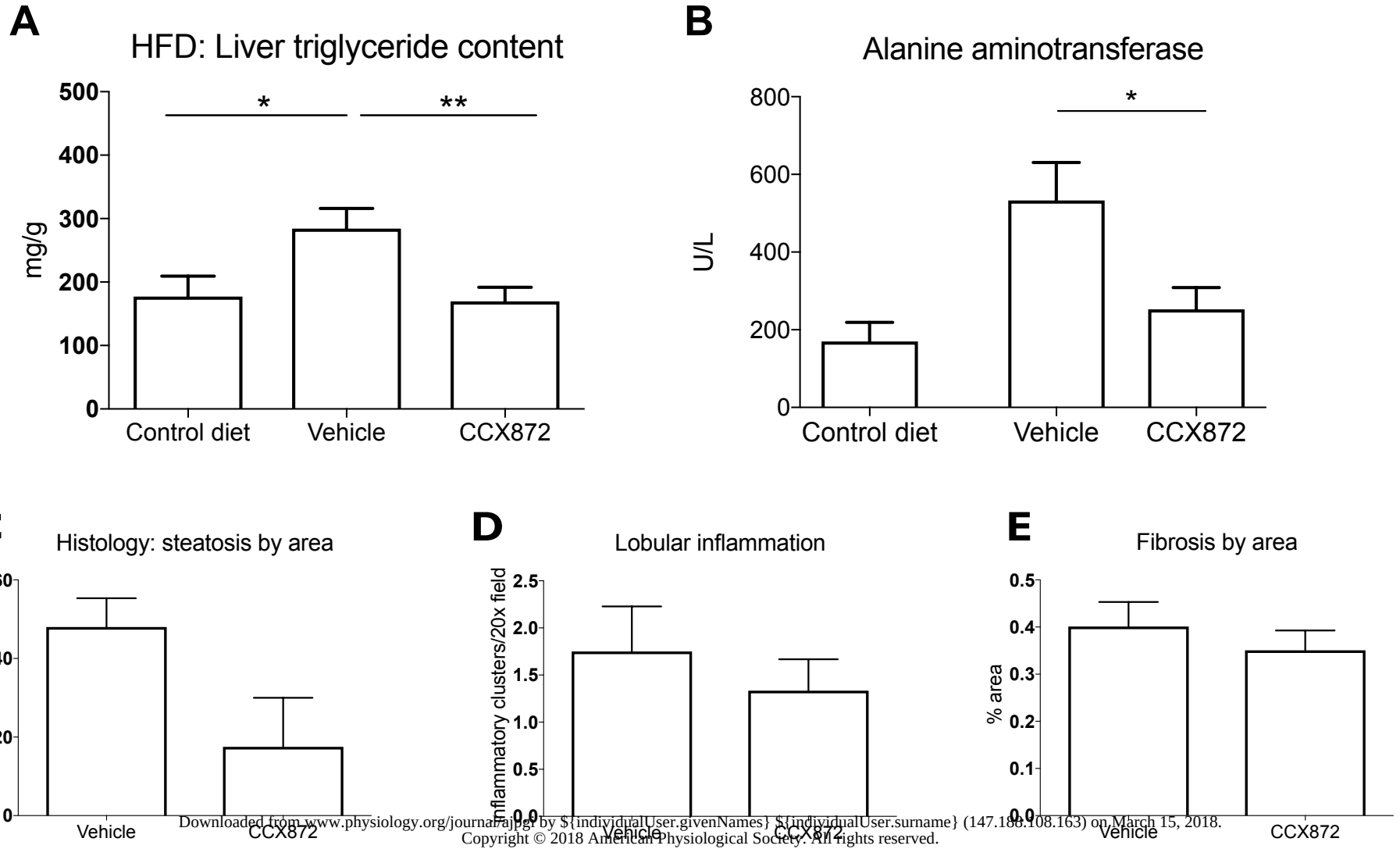

Downloaded from www.physiology.org/journal/ajpgi by ${individualUser.givenNames} ${individualUser.surname} (147.188.108.163) on March 15, 2018.
Copyright © 2018 American Physiological Society. All rights reserved.

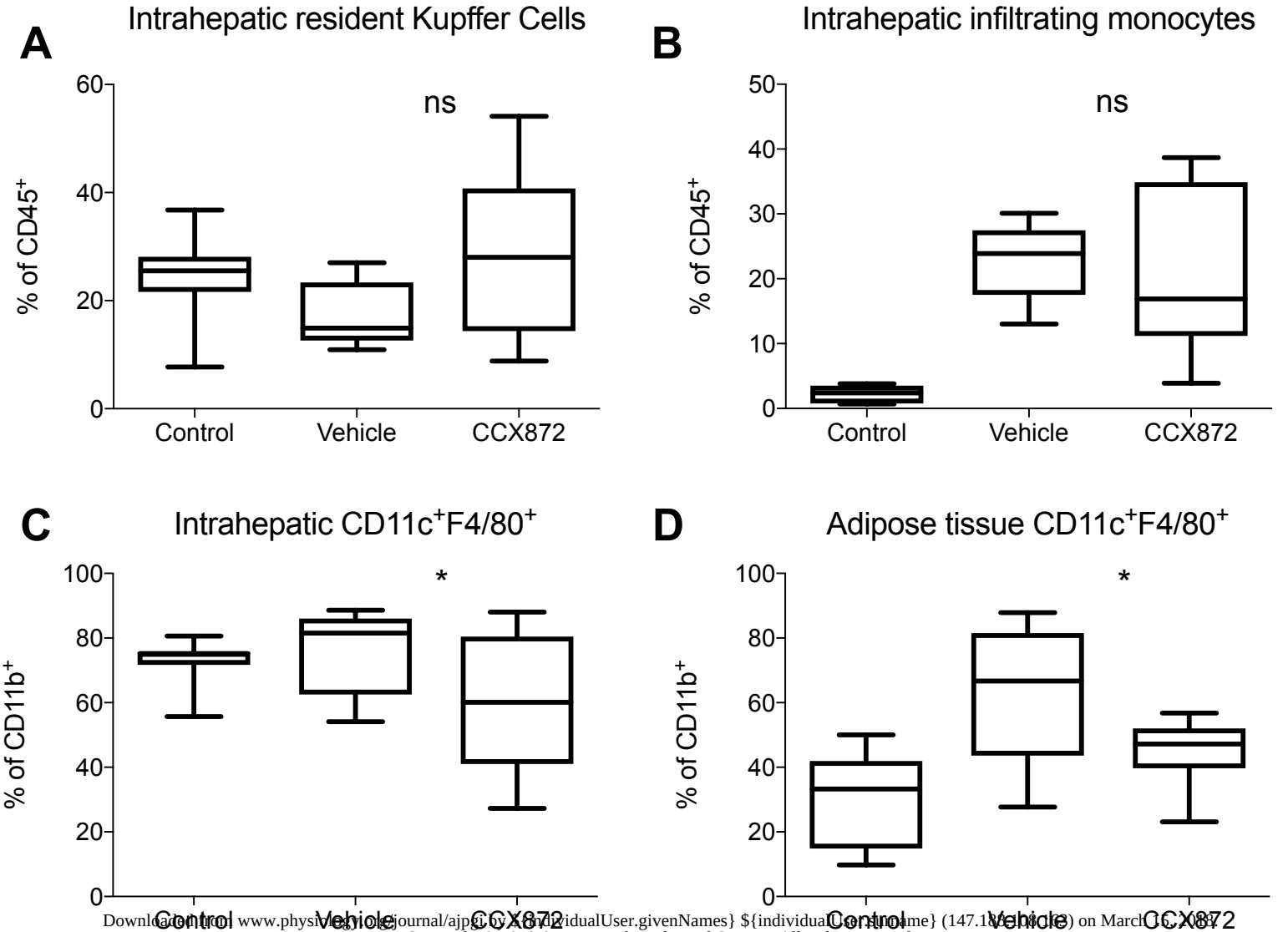

Downloaded from www.physiology.org/journal/ajpgi by ${individualUser.givenNames} ${individualUser.surname} (147.188.8.8) on March 6, 2018.
Copyright © 2018 American Physiological Society. All rights reserved.

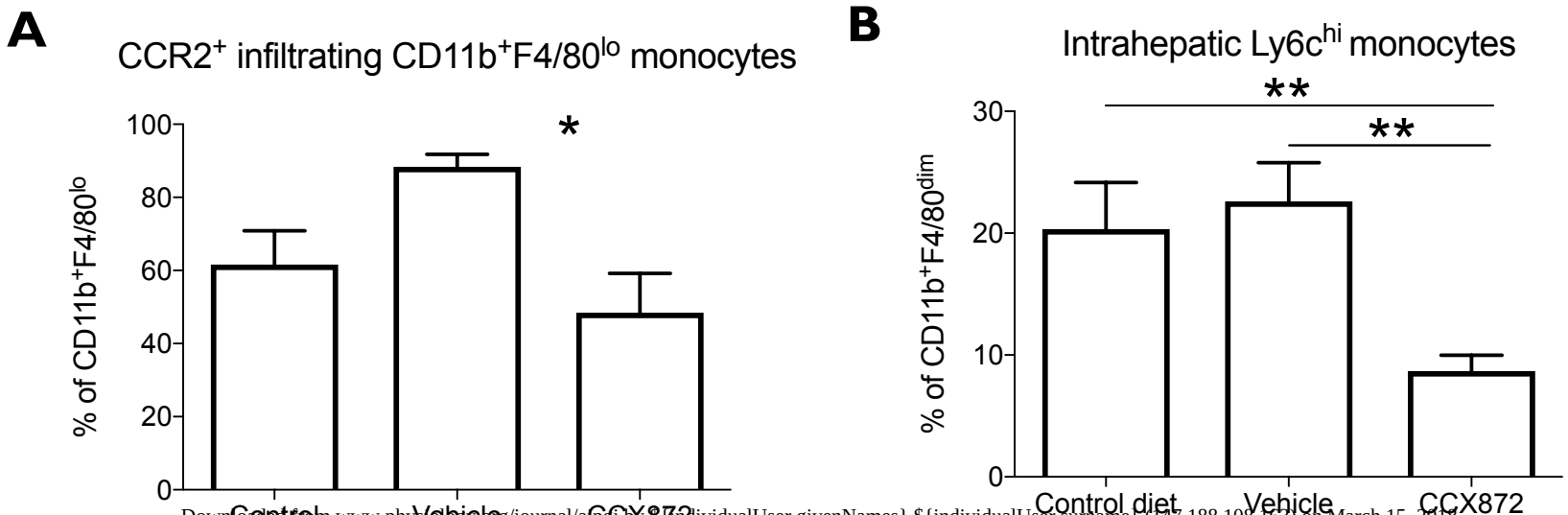

Downloaded from www.physiology.org/journal/ajpgi by ${individualUser.givenNames} ${individualUser.surname} (147.188.108.163) on March 15, 2018.
Copyright © 2018 American Physiological Society. All rights reserved.

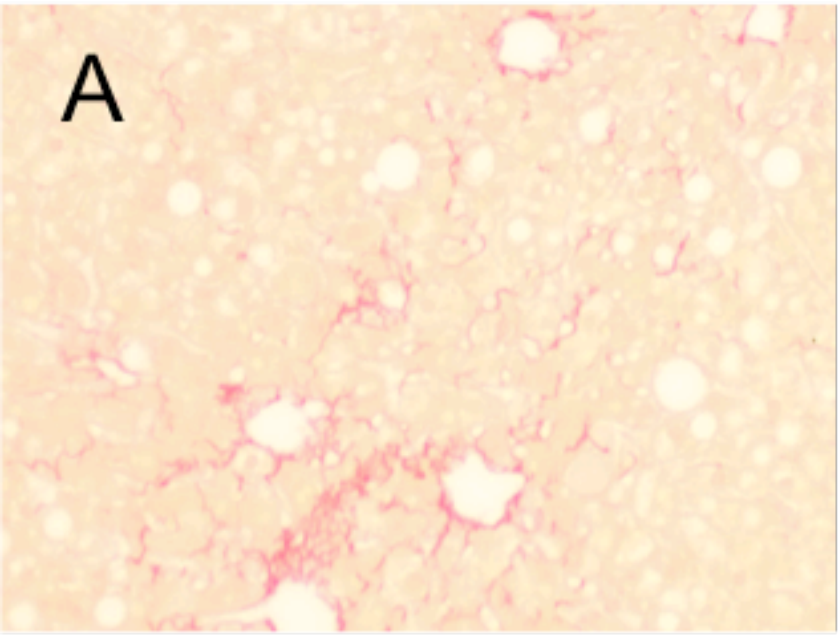

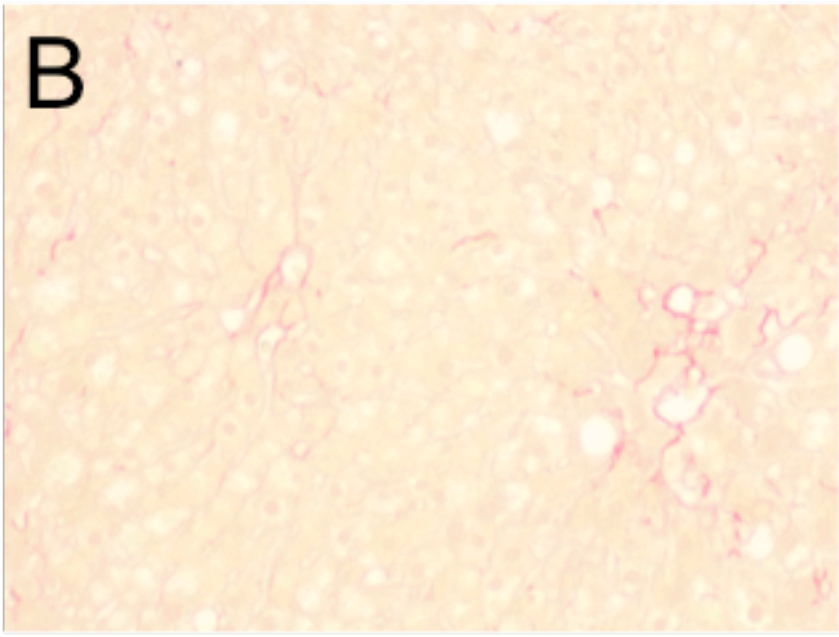

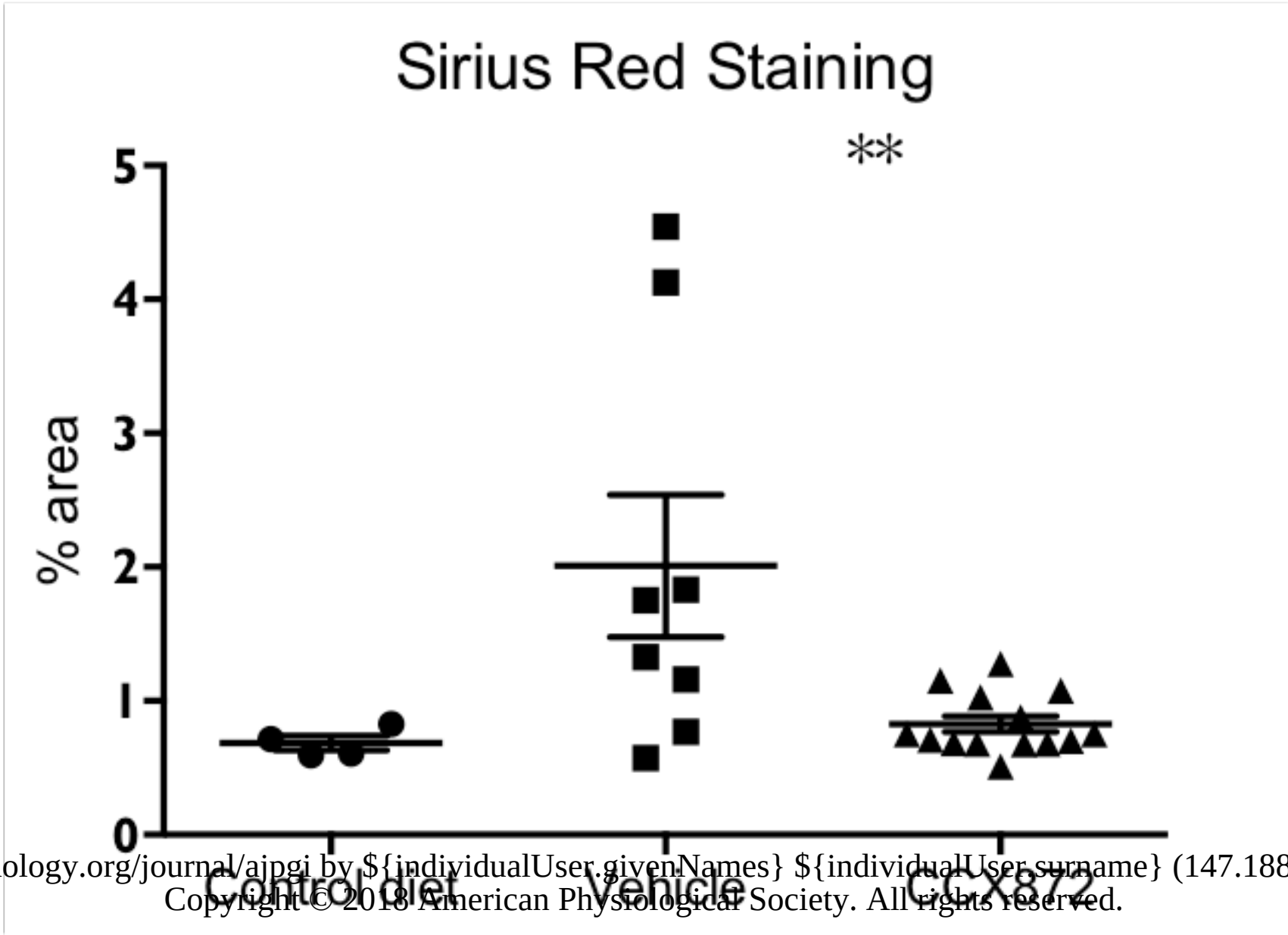

ology.org/journal/ajpgi by ${individualUser.givenNames} ${individualUser.surname} (147.188
Copyright © 2018 American Physiological Society. All rights reserved.

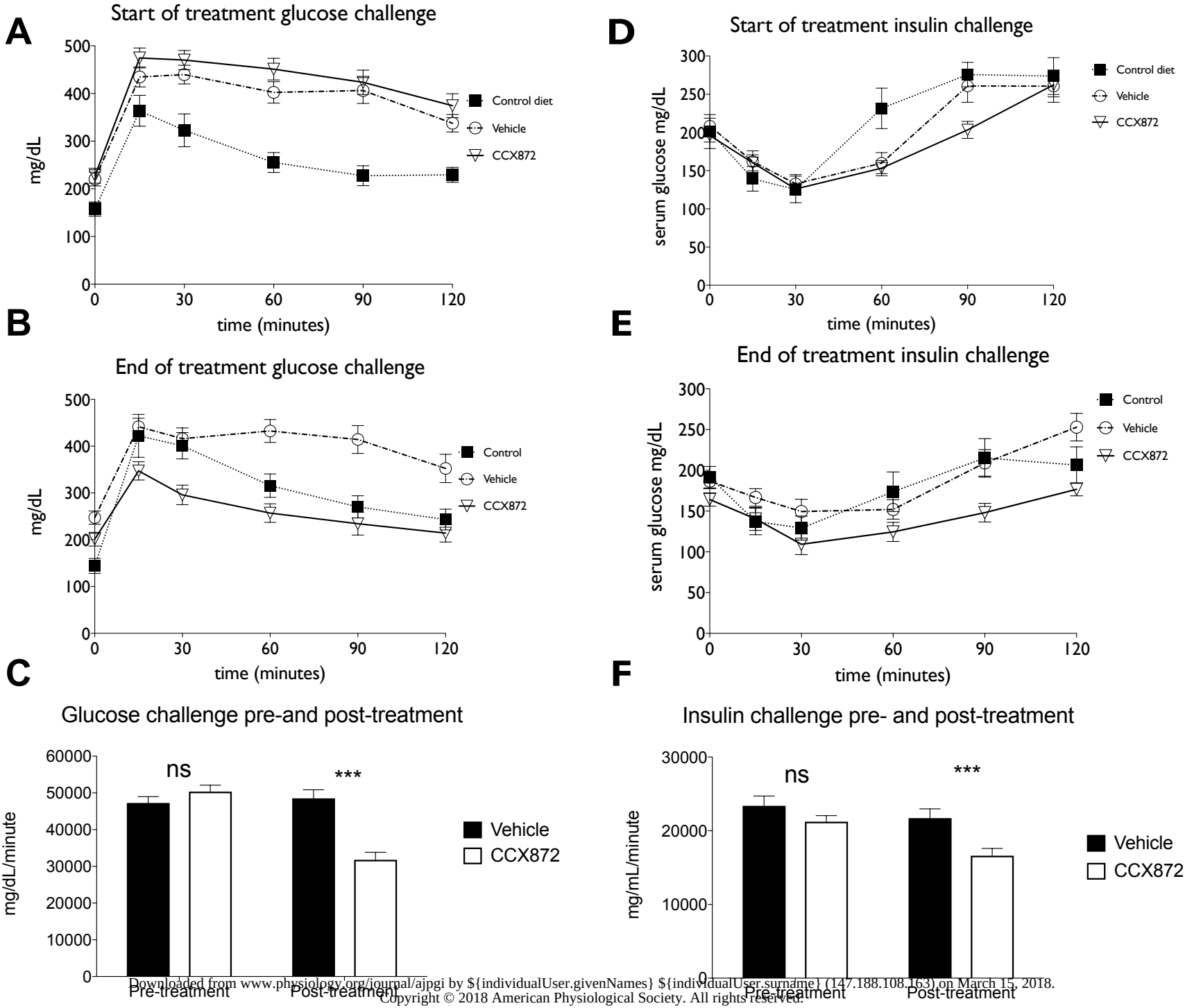

Downloaded from www.physiology.org/journal/ajpgi by ${individualUser.givenNames} ${individualUser.surname} (147.188.108.163) on March 15, 2018.
Copyright © 2018 American Physiological Society. All rights reserved.